Effective Removal of Cr(VI) from Aqueous Solution Using Modified Orange Peel Powder: Equilibrium and Kinetic Study

L. P. Liang*, Q. Wang*, F. F. Xi*, W. S. Tan*, Y. T. Zhang*, L. B. Cheng*, Q. Wu*, Y. Y. Xue* and X. Meng†**

*School of Civil Engineering, College of Life Science, College of Textile and Garment, Shaoxing University, Shaoxing, 312000, P.R.China
**Key Laboratory of Clean Dyeing and Finishing Technology of Zhejiang Province, Shaoxing University, Shaoxing, 312000, P.R.China
†Corresponding author: Xu.Meng; Mengxu0@163.com

ABSTRACT

A new adsorbent modified from orange peel (OP) was successfully synthesized by ethylenediamine crosslinking method to remove Cr(VI) from wastewater. The modified orange peel powder (MOPP) was investigated in a batch adsorption system, including both equilibrium adsorption isotherms and kinetics. Effects of several factors, including adsorbent dose, initial pH and Cr(VI) concentration were studied. The data indicated that the pH was not an essential factor that affected the adsorption process, it has a wide pH range from 4 to 10, and high adsorbent dose and lower Cr(VI) concentration could increase the Cr(VI) removal efficiency. Equilibrium data were analysed using the Langmuir, Freundlich and Temkin isotherm models and found to be well represented by the Langmuir isotherm model. The maximum capacity (q_{max}) obtained from Langmuir model was 52.08 mg/g at pH 6.0. The kinetics of adsorption followed the pseudo-second-order kinetic equation. The results suggest that MOPP is an inexpensive and efficient adsorbent for removing Cr(VI) from aqueous solution.

INTRODUCTION

The chromium ion is ubiquitous in surface and groundwater since it is widely used in industries such as plastics, pigments, wood preservatives, electroplating, leather tanning, cement, mining, dyeing and fertilizers (Altundogan et al. 2005, Gu et al. 2013). Chromium is mainly present in the form of trivalent chromium and hexavalent chromium in the aquatic environment, in which Cr(III) tend to form precipitation, low mobility and low toxicity. On the contrary, Cr(VI) is soluble in water, easy to migrate and toxic, which is one of the three internationally recognized carcinogenic metals and one of the eight most harmful chemicals to human beings (Hu et al. 2016). Hexavalent chromium can precipitate some proteins in human blood, causing anaemia, nephritis, neuritis and other diseases. Long-term contact with hexavalent chromium can also cause respiratory tract inflammation and induce lung cancer (Kota et al. 2000). According to the recommendation of the World Health Organization (WHO), the maximum allowable limit of hexavalent chromium in drinking water is 0.05 mg/L. Therefore, considering the protection of aquatic environments and requirement on the discharge limits, it is of significant importance to reduce the Cr(VI) concentration in various sources before they are discharged into water (Zhou et al. 2015).

At present, the removal methods of hexavalent chromium in sewage include chemical precipitation, ion exchange, reverse osmosis, electrochemical generation, and photocatalytic oxidation. However, these processes are difficult to be accepted due to their high cost, low efficiency, secondary pollution and unsuitability for multiple pollutants. Among these methods, adsorption technology is one of the most effective methods to remove heavy metals in water. Recently, the search for low-cost adsorbents that have metal-binding capacity has intensified. Materials locally available in large quantities such as natural materials, agricultural wastes or industrial by-products can be used as low-cost adsorbents. Some of the reported biosorbents include crab shell, wheat straw, rice straw, grape bagasse, orange waste and so on. However, to use the biomass directly may suffer from lack of specificity and poor adsorption capacity. It is observed that appropriate modification of the raw adsorbents by crown esters, amines, polyethylamine and sulphur bearing groups can eliminate the drawbacks and improve their performances significantly (Mukhopadhyay et al. 2006).

The orange peel (OP) is a quite abundant agricultural waste which can be reused as adsorbent. The valuable waste material orange peel (OP) principally consists of cellulose, pectin, hemicellulose, lignin, chlorophyll pigments and

other low molecular weight hydrocarbons (Feng et al. 2008). Cellulose, hemicellulose, and lignin structures have a large number of easily available hydroxyl groups that can be used for the synthesis of functional polymers (Nakamura et al. 1992). World's orange production is estimated to be > 60 million tons per year (Fernandez et al. 2014). OP is abundant in juice industry residues, but many of them abandoned as waste without proper utilization. In general, the adsorption capacity of crude fruit waste is very low. Hence, in recent years, using such fruit residues as functional polymers has attracted much interest. For example, Feng et al. (2008) prepared a chemically modified orange peel adsorbent by hydrolysis of the graft copolymer, which was synthesized by the interaction of methyl acrylate and cross-linked orange peel. The results showed that the modified orange peel successfully adsorbed 289 mg.g^{-1} of Copper (II). Liang et al. (2009) succeeded in adsorbing 204.50 mg.g^{-1} Pb^{2+} in the solution by chemically modifying the original orange peel by introducing sulphur groups with the carbon disulphide treatment in alkaline medium.

This work aimed to prepare a new adsorbent which modified the orange peel (OP) by ethylenediamine crosslinking method and to study the adsorption capacity of Cr(VI). The effects of biosorbent dosage, pH, and initial Cr(VI) concentration on Cr(VI) removal in solution were investigated. Besides this, adsorption isotherms and kinetics were also discussed and different adsorption models were used to evaluate the experimental data and to illustrate the possible adsorption mechanism.

MATERIALS AND METHODS

Materials

All the chemicals used in this study were of pure analytical grade. Stock solutions of heavy metals were prepared by dissolving K$_2$Cr$_2$O$_7$ in double-distilled water and then diluted to desired concentrations. The adsorbent used in this study was prepared by collecting the fruits from a local market in Shaoxing, Zhejiang, China. N, N-dimethylformamide (C$_3$H$_7$NO), epichlorohydrin (C$_3$H$_5$ClO), ethylenediamine (C$_2$H$_8$N$_2$), triethylamine(C$_6$H$_{15}$N), and all the other reagents were purchased from the Sinopharm Group Chemical Reagent Co., Ltd., China. All these chemicals were of analytical grade and used as received.

Preparation of Cationic Adsorbent

The OP was first washed with double distilled water to remove dirt and other particulate matter, and then dried at 60°C inside a convection oven for 24 h. The dried sample was ground and sieved to the desired mesh size (100-250 mesh). To 8 g of OP were added 20 mL of epichlorohydrin and 16 mL of N, N-dimethylformamide (DMF) in a 250-mL three-neck round-bottom flask at 85°C for 1 h. Next, 6 mL of ethylenediamine was added and the mixture was stirred for 1 h at 85°C. Finally, 15 mL of 99% triethylamine (w/w) was added and stirred for 3 h at 85°C. The primary product was washed with double distilled water until the eluant was neutral, and then dried overnight at 60°C and sieved to obtain particles. The prepared MOPP was stored in a desiccator for further use.

Batch Experiments

Batch equilibrium studies were carried out by adding a fixed amount of MOPP to 250-mL sealed conical flasks containing 100 mL of different initial concentrations of Cr(VI) solution. The flasks were placed in a shaking thermostat machine at a speed of 150 r/min. Aqueous samples (5 mL) were withdrawn at equilibrium and filtered using a 0.45-μm filter. The adsorption capacities of MOPP were calculated under different environmental conditions to understand their effects on the reaction. The equilibrium adsorbed concentration, q_e (mg.g^{-1}), was determined according to the following equation:

$$q_e = \frac{(C_0 - C_e)V}{W} \qquad \ldots(1)$$

Where, C_0 and Ce (mg.L^{-1}) represent the liquid-phase concentrations of Cr(VI) initially and at equilibrium, respectively; q_e (mg.g^{-1}) is the equilibrium adsorption capacity; V (L) is the volume of the solution, and W (g) is the mass of the adsorbent. In addition, all the adsorption experiments were conducted in duplicate, and the mean values were calculated. The results were reproducible at most 5% error.

RESULTS AND DISCUSSION

Scanning Electron Microscopy Analysis

The morphology of OP and MOPP is presented in Fig. 1 (SEM image). The surface of the OP has well-structured layers without a well-defined direction, cavities and channels can be observed. These features are typical for adsorption materials. When comparing the SEM images of OP and MOPP, structural changes are evident with the latter showing a more porous and irregular surface. This led to physical and chemical cross-linking on the surface of adsorbent to enhance adsorption (Singh et al. 2014). Based on this fact, it can be determined that MOPP present an adequate morphology for metal adsorption.

FTIR Spectroscopy Analysis

Fourier transform infrared spectroscopy (FTIR) was used to identify the functional groups responsible for Cr(VI) uptake.
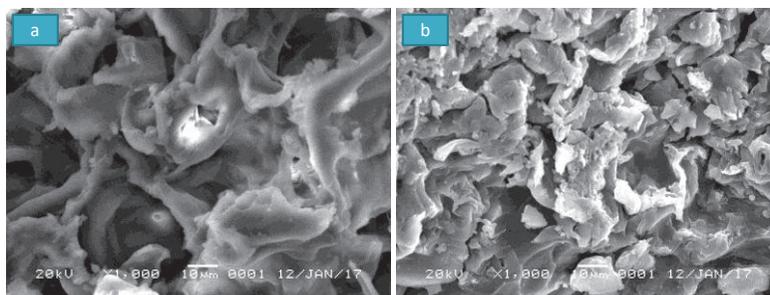
Fig. 1: SEM images of OP (a) and MOPP (b) of magnifications of 1000 times.

The infrared spectra of OP and MOPP are shown in Fig. 2. In OP spectrum, at a wavelength of about 3420 cm^{-1}, the broad and strong absorption peak corresponds to the O-H tensile vibration of alcohols, which stretching vibration region is from 3750cm^{-1} to 3000cm^{-1}. The compositions of OP, like hemicellulose, cellulose, pectin and lignin including phenols and carboxylic acids indicate the presence of "free" hydroxyl groups on the surface of the adsorbent (Gnanasambandam et al. 2000). The peak at 2912 cm^{-1} is caused by the C-H stretching vibration on the saturated carbon in the aliphatic acids. The peak observed at 2368 cm^{-1} may be is the area of triple bond and a cumulative double bond. The absorption of carboxyl group occurs most often in the region of 1755-1670 cm^{-1}, therefore, the peak in the spectrum is corresponding to the tensile vibration of the bond caused by non-ionic oxycar-byl (-COOH, -COCH3) (Say et al. 2003). The peaks at 1644 cm^{-1} and 1520 cm^{-1} are located in the double bond telescopic vibration region, which mainly includes the stretching vibration of carbon-carbon double bond, carbon-nitrogen double bond, nitrogen-nitrogen double bond, etc. The 1060 cm^{-1} peak may be caused by the stretching vibration of C-OH of ethanol group and carboxylic acid (Sengil & Ozacar 2009).

Compared with OP, the spectrum of MOPP after modifica-tion can be seen that the peak caused by the C-H stretching vibration is not obvious. Carboxyl peak was disappeared around 1752 cm^{-1} and a new peak was discovered at 1647 cm^{-1}. This shows that some functional groups have been successfully modified.

Effect of solution initial pH

Solution pH is an important controlling parameter that strongly influences the adsorption of metals onto the sol-id-liquid interface (Chen et al. 2010). Batch adsorption experiments were carried out by varying the pH between 4.0 and 10.0 under optimized conditions of 200 mg.L^{-1} initial concentration and 1 g.L^{-1} MOPP to identify the Cr(VI) uptake capacity of the adsorbent, and the results are shown in Fig. 3. At this pH range, the Cr(VI) sorption capacity of MOPP was all above 22.32 mg.L^{-1}, and the maximum adsorption occurred at pH 6.0 (25.76 mg.g^{-1}). It could be seen from the figure that pH was not a considerable factor in this study, which makes it economical for wastewater treatment. The most effective pH was found to be 6.0 and it was used in further studies.
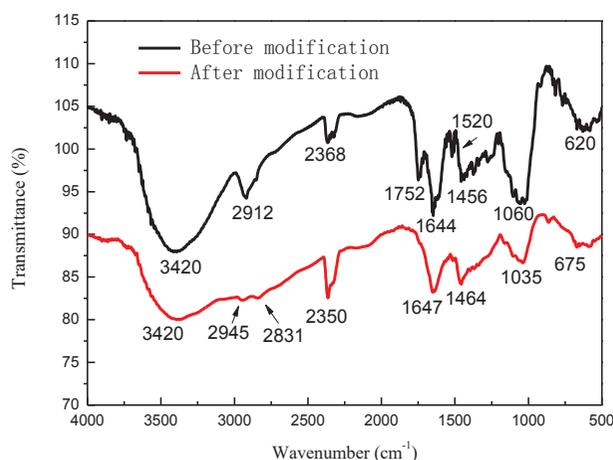
Fig. 2: FT-IR spectra of orange peel before and after modification by ethylenediamine.
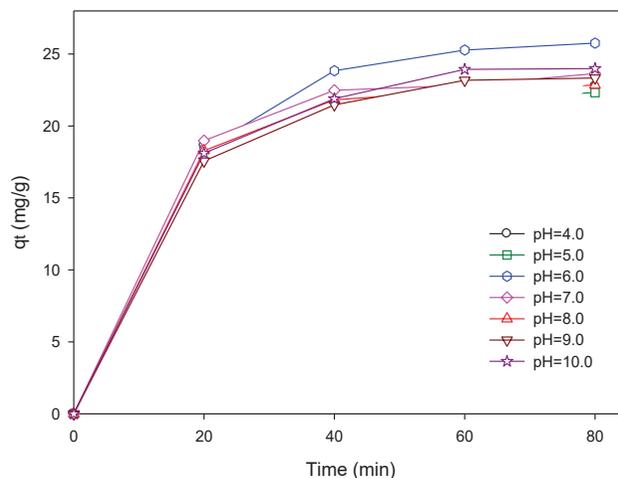
Fig. 3: Effect of pH on the kinetics of Cr(VI) removal by cation adsorbent.

Effect of adsorbent dose

The effect of the adsorbent dosage on the removal of Cr(VI) in solution was investigated under the conditions of pH 6 and 200 mg.L^{-1} solution concentration. The results are shown in Fig. 4. The removal amount of Cr(VI) ions increased significantly from 23.22 to 28.01 mg.g^{-1}, with adsorbent concentration increasing from 1 to 3 g.L^{-1}. With increasing adsorbent concentration, greater surface area and more adsorption sites became available for adsorption, and almost all the Cr(VI) ions were adsorbed when the concentration was increased to 3 g.L^{-1}. So, it could be concluded that further increasing the concentration, and when it reached 3 g.L^{-1}, had a negligible effect on Cr(VI) removal.

Effect of Contact Time and Initial Concentration

The adsorption of Cr(VI) onto MOPP at different initial concentrations was studied as a function of time to determine the point of equilibrium under the condition of pH 6 and 2 g.L^{-1} MOPP, as shown in Fig. 5. The adsorption capacity increased with increasing Cr(VI) ions concentration in the medium, and when the initial Cr(VI) concentration increased from 50 to 600 mg.L^{-1}, the Cr(VI) uptake capacity of the MOPP increased from 5.39 to 59.43 mg.g^{-1}. This may be attributed to the higher initial Cr(VI) concentration leading to faster and more strongly binding sites compared to lower concentrations of Cr(VI) at the same dose of adsorbent (Baral et al. 2009). It was also observed that adsorption of Cr(VI) ions onto MOPP was rather quick, and after 60 min, complete adsorption equilibrium was obtained. For the sake of the combined experiments, all further studies were carried out for 90 min. The initially higher rate was probably due to the high affinity of the interacting groups on the surface of MOPP. Once the exterior surface reached saturation, the Cr(VI) ions penetrated through the pores and were adsorbed inside them. Besides, the curves were single, smooth, and
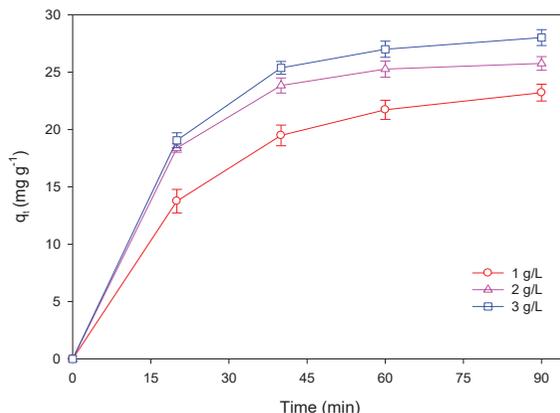
Fig. 4: Effect of cation adsorbent dose on the kinetics of Cr(VI) removal by cation adsorbent.
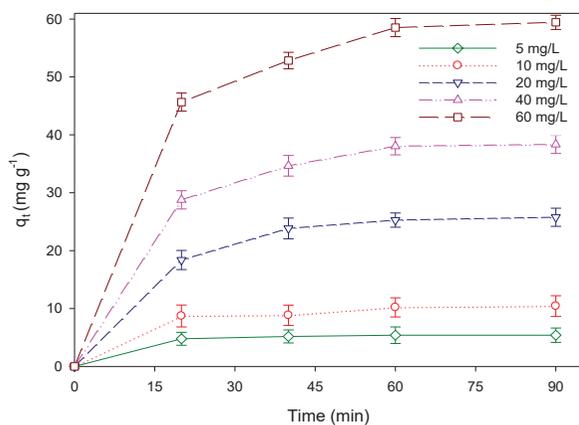
Fig. 5: Effect of initial Cr(VI) concentration on the kinetics of Cr(VI) removal by cation adsorbent.

continuous toward saturation, indicating the formation of monolayer coverage of Cr(VI) on the MOPP surface (Lugo-Lugo et al. 2012).

Adsorption Kinetics Study

Adsorption kinetics is one of the most essential characteristics which govern the solute uptake rate; it represents the

Fig. 6: Simulated results of pseudo-first-order kinetics (a); pseudo-second-order kinetics (b) at different initial Cr(VI) concentrations.

adsorption capacity of the adsorbent and therefore, determines its potential applications. It could be seen from Fig. 6(a) and (b) that with the increase of initial concentration, more Cr(VI) was adsorbed onto the MOPP, also the time to achieve adsorption equilibrium was prolonged. However, it still can be concluded that all the adsorption processes proceed rapidly and this observed rapid kinetics has significant practical importance as it could be used for the scale-up to a larger system.

The kinetic experiments were carried out and data were fitted into the pseudo-first-order, pseudo-second-order and intraparticle diffusion models respectively. The pseudo-first-order model is represented by the following equation (Chairat et al. 2006):

$$\log(q_e - q_t) = \log q_e - \frac{k_1}{2.303}t \qquad …(2)$$

Where, q_e (mg.g^{-1}) and q_t (mg.g^{-1}) are the amounts of Cr(VI) adsorbed at equilibrium (mg.g^{-1}) and at time t (min), respectively, and k_1 is the rate constant of pseudo-first-order adsorption process (min^{-1}). Values of k_1 and equilibrium adsorption density q_e at 25°C were calculated from the plots of $\log(q_e - q_t)$ versus t for different initial concentrations of Cr(VI). The pseudo-second-order kinetic model can be expressed as (Ho et al. 1998):

$$\frac{t}{q_t} = \frac{1}{k_s q_e^{2}} + \frac{1}{q_e}t \qquad …(3)$$

Where, k_2 (g mg^{-1} min) is the rate constant for the pseudo-second-order adsorption kinetics. Values of k_2 and q_e for different initial concentrations of Cr(VI) were calculated from the slope and intercept of the linear plot of t/q_t versus t. The plot of t/q_t versus t at 25°C is shown in Fig. 6 (b).

The modelled parameters from pseudo-first and pseudo-second-order adsorption kinetic equations and the intraparticle diffusion equation are given in Table 1. The linear plots of t/q_t versus t indicated a good agreement between the experimental and calculated q_e values for different initial Cr(VI) concentrations. Furthermore, the correlation coefficients of the pseudo-second-order kinetic model ($R^2 = 0.9802$) were greater than that of the pseudo-first-order model ($R^2 = 0.9105$), which indicated that the pseudo-second-order was more suitable for describing the adsorption of Cr(VI) on MOPP. This strongly suggested that the reaction between Cr(VI) and MOOP was chemical adsorption or chemisorption (Suksabye et al. 2008). A similar phenomenon has been observed in Cr(VI) adsorption by used coir pith (Suksabye et al. 2008), *Leersia hexandra* biomass (Li et al. 2009), and ethylenediamine-modified rice hull (Tang et al. 2003).
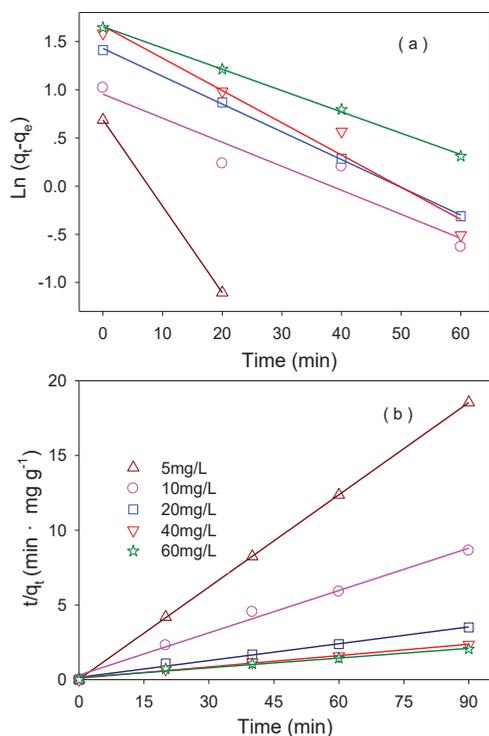
Adsorption Isotherm Analysis

Modelling of adsorption isotherm data is important for predicting and comparing composite adsorption properties of the adsorbent. It provides a comprehensive understanding of the nature of the interaction (Mahmoodian et al. 2015). In this study, three important isotherms were applied to fit the equilibrium data: the Langmuir, Freundlich and Temkin isotherms.

Based on the assumption that all the adsorption sites are equivalent and adsorption in active sites is independent of whether the adjacent is occupied, the Langmuir adsorption model can be expressed as (Bhugun et al. 1997):

$$\frac{1}{q_e} = \frac{1}{q_m} + \frac{1}{K_L q_m C_e} \qquad \qquad …(4)$$

Where, q_e is the amount of adsorbate adsorbed per unit mass of adsorbent at equilibrium (mg.g^{-1}), q_m is the monolayer capacity of the adsorbent (mg.g^{-1}), and K_L is the adsorption constant (L mg^{-1}). According to this equation, a plot of $1/q_e$ versus $1/C_e$ gives a straight line of slope $1/q_m$ and intercepts $1/(q_m K_L)$.

The well-known logarithmic form of the Freundlich isotherm is expressed by the following equation (Elzinga et al 1999):

$$Ln q_e = Ln K_F + \frac{1}{n} Ln C_e \qquad \qquad …(5)$$

Where, K_F and n are Freundlich constants related to adsorbent capacity and the sorption intensity of the adsorbent, respectively. Temkin isotherm takes into account sorbate-adsorbent interactions and assumes that fall in the heat of adsorption is linear rather than logarithmic. The Temkin isotherm can be expressed in its linear form (Samia et al. 2016) as:

$$q_e = B Ln A + B Ln C_e \qquad \qquad …(7)$$

Table 1: Comparisons of rate constants and calculated q_e by the pseudo-first-order kinetics, pseudo-second-order kinetics at different initial Cr(VI) concentrations.

ρ Cr(VI) (mg.L^{-1})	Experiment q_e(mg.g^{-1})	Pseudo-first-order kinetics			Pseudo-second-order kinetics		
		R^2	q_e	K_1(g mg^{-1} min^{-1})	R^2	q_e	K_2(g mg^{-1} min^{-1})
5	4.8533	1.0000	4.8529	0.2063	1.0000	4.8614	1.6088
10	10.4322	0.9105	8.9681	0.0573	0.9923	10.5932	0.0285
20	25.7601	0.9995	26.6747	0.0663	0.9913	26.6667	0.0093
40	38.3487	0.9606	45.6457	0.0769	0.9930	39.5257	0.0069
60	43.9631	0.9989	44.9159	0.0509	0.9802	46.0829	0.0034

Table 2: Langmuir, Freundlich and Temkin model constants and correlation coefficients for Cr(VI) removal by cation adsorbent at 25°C.

Temperature	Langmuir			Freundlich			Temkin		
	R^2	q_m	K_L(L.mg^{-1})	R^2	K_F(mg^{1-n}L^{n}g^{-1})	N	R^2	A (L.mg^{-1})	B
25°C	0.9915	52.0833	0.0606	0.9626	3.1606	0.6763	0.9826	1.8125	26.8822

Table 3: Adsorption capacities of various adsorbents for Cr(VI).

Adsorbent (g.L^{-1})	Major reaction conditions	Q$_m$ (mg.g^{-1})	Source of information
MOPP	[Cr(VI)]$_0$ = 200 mg.L^{-1},[Adsorbent]$_0$ = 2 g.L^{-1}, T = 293-303 K, pH = 6, reaction time = 90 min	52.08	The data from this paper
Wheat straw	[Cr(VI)]$_0$ = 11 mg.L^{-1},[Adsorbent]$_0$ = 1g.L^{-1}, T = 298 K, pH = 2, reaction time = 60 min	9.19	(Samia et al. 2016)
aminated rice straw-grafted-poly	[Cr(VI)]$_0$ = 100 mg.L^{-1},[Adsorbent]$_0$ = 0.5 g.L^{-1}, T = 333 K, pH = 2, reaction time = 60 hours	140.39	(Lin et al. 2018)
Corn cob ash	[Cr(VI)]$_0$ = 500 mg.L^{-1},[Adsorbent]$_0$ = 20g.L^{-1}, T = 297-299K, pH = 6.2, reaction time = 24 hours	4.2	(Singh et al. 2014)
Orange peel powder	[Cr(VI)]$_0$ = 500 mg.L^{-1},[Adsorbent]$_0$ = 20g.L^{-1}, T = 297-299 K, pH = 6.2, reaction time = 24 hours	10.2	(Singh et al. 2014)
Sawdust	[Cr(VI)]$_0$ = 5 mg.L^{-1},[Adsorbent]$_0$ = 10 g.L^{-1}, T = 298 K, pH = 6, reaction time = 6 hours	3.3	(Srivastava et al. 1986)
Sugar cane bagasse	[Cr(VI)]$_0$ = 100 mg.L^{-1}, [Adsorbent]$_0$ = 4 g.L^{-1},T = 298 K, pH = 1.2, reaction time = 24 hours	13.4	(Sharma et al. 1994)

Where, A is the equilibrium binding constant corresponding to the maximum binding energy (L.mg^{-1}) and B is the Temkin constant related to the heat of adsorption.

From the plot of Lnq_e versus LnC_e, the intercept and slope give the values of K_F and n. Fig. 7(a)(b) shows Langmuir and Freundlich adsorption isotherms of MOPP at 25°C. It was clear from Fig. 7(a)(b) that data fitted better to Langmuir
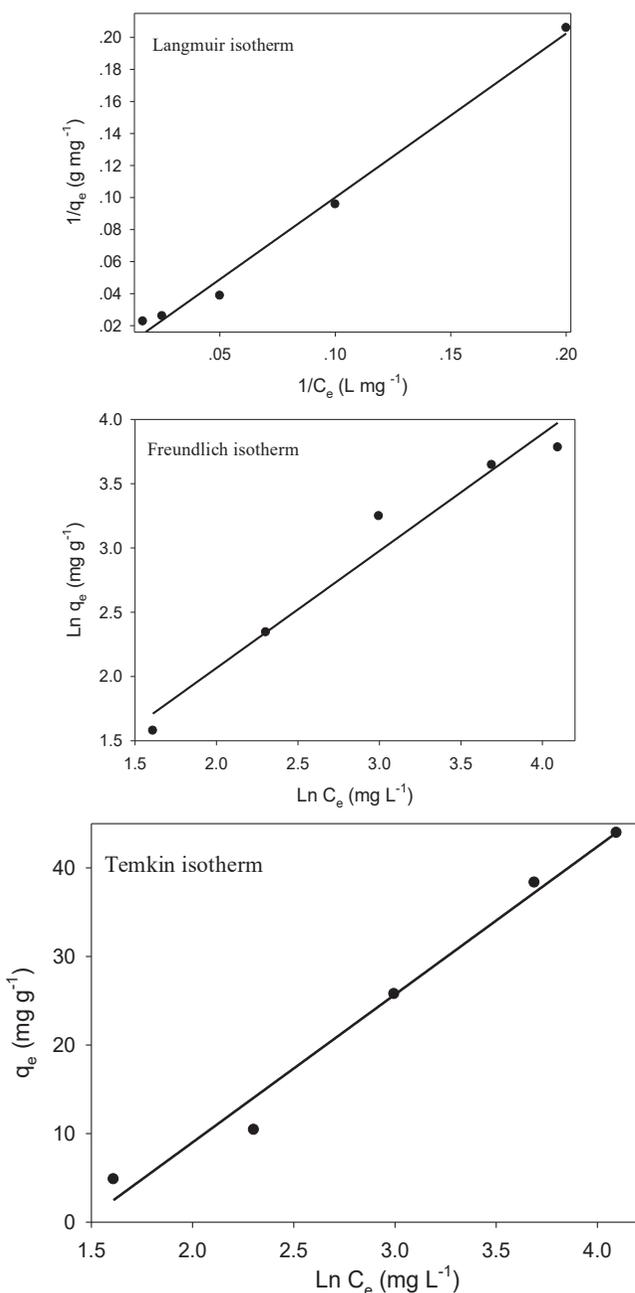
model in comparison to the Freundlich model. This indicated the monolayer adsorption on the homogeneous surface of the MOPP adsorbent with identical binding sites. The constants A and B were calculated from the slope and intercept of q_e versus LnC_e. From linear regression, the R^2 values of 0.8746 for MOPP (Table 2), were also lower than Langmuir values. Therefore, the adsorption of MOPP was found to be well represented by the Langmuir adsorption isotherms, and the maximum adsorption capacity of MOPP was 52.08 mg.g^{-1} calculated by it. In addition, we compared the adsorption capacity of other materials to Cr(VI), and found that MOPP has a good removal effect. The specific information is given in Table 3.

CONCLUSION

The potential of modified orange peel (MOPP) for removing Cr(VI) from aqueous solutions was studied in the present work. Batch experiments showed it an effective adsorbent for removal Cr(VI) from aqueous solution. The amount of Cr(VI) adsorbed was found to vary with initial solution pH, initial Cr(VI) concentrations, contact time, and adsorbent dose. Acidic pH was found to enhance the Cr(VI) removal the least. After fitting and analysing the data, it was found that the adsorption reaction between MOPP and Cr(VI) accorded with pseudo-second-order kinetics and was also presented well by the Langmuir adsorption isotherms. The maximum monolayer adsorption capacity of Cr(VI) was 52.08 mg.g^{-1} at an optimum pH of 6.0. Based on the results, it could be concluded that MOPP is an effective and efficient adsorbent for the removal of Cr(VI) from aqueous solutions.

ACKNOWLEDGEMENTS

REFERENCES

Altundogan, H.S. 2005. Cr(VI) removal from aqueous solution by iron (III) hydroxide-loaded sugar beet pulp. Process Biochem., 40(3-4): 1443-1452.

Baral, S.S., Das, N., Chaudhury, G.R. and Das, S.N. 2009. A preliminary study on the adsorptive removal of Cr(VI) using seaweed, *Hydrilla verticillata*. J. Hazard. Mater., 171(1-3): 358-369.

Bhugun, I. and Anson, F.C. 1997. A generalized treatment of the dynamics of the adsorption of Langmuirian systems at stationary or rotating disk electrodes1. J. Electroanal. Chem., 439(1): 1-6.

Chairat, M., Rattanaphani, S., John, B.B. and Rattanaphani, V. 2006. Adsorption kinetic study of lac dyeing on cotton. Dyes Pigm., 76(2): 435-439.

Fig. 7: Simulated results of Langmuir (a), Freundlich (b), Temkin (c) isotherm for Cr(VI) removal by cation adsorbent at 25°C.

Chen, S., Yue, Q., Gao, B. and Xu, X. 2010. Equilibrium and kinetic adsorption study of the adsorptive removal of Cr(VI) using modified wheat residue. J. Colloid Interface Sci., 349(1): 256-264.

Elzinga, E.J., Grinsven, J.J.M.V. and Swartjes, F.A .1999. General purpose Freundlich isotherms for cadmium, copper and zinc in soils. Eur. J. Soil. Sci., 50(1): 139-149.

Feng, N., Guo, X. and Liang, S. 2008. Adsorption study of copper (II) by chemically modified orange peel. J. Hazard. Mater., 164(2-3): 1286-1292.

Fernandez, M.E., Nunell, G.V., Bonelli, P.R. and Cukierman, A.L. 2014. Activated carbon developed from orange peels: Batch and dynamic competitive adsorption of basic dyes. Ind. Crops. Prod., 62: 437-445.

Gnanasambandam, R. and Proctor, A. 2000. Determination of pectin degree of esterification by diffuse reflectance Fourier transform infrared spectroscopy. Food Chem., 68(3): 327-332.

Gu, H., Rapole, S.B., Huang, Y., Cao, D.M., Luo, Z.P., Wei, S. and Gao, Z. 2013. Synergistic interactions between multi-walled carbon nanotubes and toxic hexavalent chromium. J. Mater. Chem. A., 1(6): 2011-2021.

Ho, Y.S. and Mckay, G. 1998. The kinetics of sorption of basic dyes from aqueous solution by sphagnum moss peat. Can. J. Chem. Eng., 76(4): 822-827.

Hu, J., Lin, Y. and Zhu, G. 2016. Review on migration and transformation mechanisms of chromium in the subsurface and remediation techniques for chromium- contaminated sites. Environ. Eng., 34(S1): 1053-1056.

Kota , J. and Stasicka, Z. 2000. Chromium occurrence in the environment and methods of its speciation. Environ. Pollut., 107(3): 263-283.

Li, J., Lin, Q., Zhang, X. and Yan, Y. 2009. Kinetic parameters and mechanisms of the batch biosorption of Cr(VI) and Cr (III) onto *Leersia hexandra* Swartz biomass. J. Colloid Interface Sci., 333(1): 71-77.

Liang, S., Guo, X., Feng, N. and Tian, Q. 2009. Application of orange peel xanthate for the adsorption of Pb^{2+} from aqueous. J. Hazard. Mater., 170(1): 425-429.

Lin, C., Luo, W., Lou, T., Zhou, Q., Li, H. and Jing, L. 2018. A study on adsorption of Cr(VI) by modified rice straw: Characteristics, performances and mechanism. J. Cleaner Prod., 196: 626-634.

Lugo-Lugo, V., Barrera-Díaz, C., Ureña-Núñez, F., Bilyeu, B. and Linares-Hernandez, I. 2012. Biosorption of Cr (III) and Fe (III) in single and binary systems onto pretreated orange peel. J. Environ. Manage.,

112: 120-127.

Mahmoodian, H., Moradi, O., Shariatzadeha, B., Salehf , T.A., Tyagi, I., Maity, A., Asif, M. and Gupta, V.K. 2015. Enhanced removal of methyl orange from aqueous solutions by poly HEMA-chitosan-MWCNT nano-composite. J. Mol. Liq., 202: 189-198.

Mukhopadhyay, B., Sundquist, J. and White, E. 2006. Hydro-geochemical controls on removal of Cr(VI) from contaminated groundwater by anion exchange. Appl. Geochem., 22(2): 380-387.

Nakamura, S., Amano, M., Saegusa, Y. and Sato, T. 1992. Preparation of aminoalkyl celluloses and their adsorption and desorption of heavy metal ions. J. Appl. Polym. Sci., 45(2): 265-271.

Samia, R., Mounir, B. and Salah, H. 2016. Neuro-fuzzy modeling of Cu(II) and Cr(VI) adsorption from aqueous solution by wheat straw. Desalin. Water Treat., 57(14): 1-16.

Say, R., Emir Diltemiz, S., Garipcan, B., Patir, S. and Denizli, A. 2003. Novel methacryloylamidophenylalanine functionalized porous chelating beads for adsorption of heavy metal ions. Adv. Polym. Technol., 22: 355-364.

Sengil, I., Ayhan and Ozacar, M. 2009. Competitive biosorption of Pb^{2+} Cu^{2+} and Zn^{2+} ions from aqueous solutions onto valonia tannin resin. J. Hazard. Mater., 166(2-3): 1488-1494.

Sharma, D.C. and Forster, C.F. 1994. A preliminary examination into the adsorption of hexavalent chromium using low-cost adsorbents. Bioresour. Technol., 47(3): 257-264.

Singh, R. 2014. Comparison of hexavalent chromium adsorption from aqueous solutions by various biowastes and granulated activated carbon. Indian Chem. Eng., 56(1): 12-28.

Srivastava, H.C.P., Mathur, R.P. and Mehrotra, I. 1986. Removal of chromium from industrial effluents by adsorption on sawdust. Environ. Technol., 7(1-12): 55-63.

Suksabye, P., Nakajima, A., Thiravetyan, P., Baba, Y. and Nakbanpote, W. 2008. Mechanism of Cr(VI) adsorption by coir pith studied by ESR and adsorption kinetic. J. Hazard. Mater., 161(2-3): 1103-1108.

Tang, P.L., Lee, C.K., Low, K.S. and Zainal, Z. 2003. Sorption of Cr(VI) and Cu(II) in aqueous solution by ethylenediamine modified rice hull. Environ. Technol., 24(10): 1243-1251.

Zhou, J., Wang, Y., Wang, J., Qiao, D., Long, D. and Ling, L. 2015. Effective removal of hexavalent chromium from aqueous solutions by adsorption on mesoporous carbon microspheres. J. Colloid Interf. Sci., 462(8): 200.